

Son Xuat Ta, Ikmo Park, and Richard W. Ziolkowski

Crossed Dipole Antennas

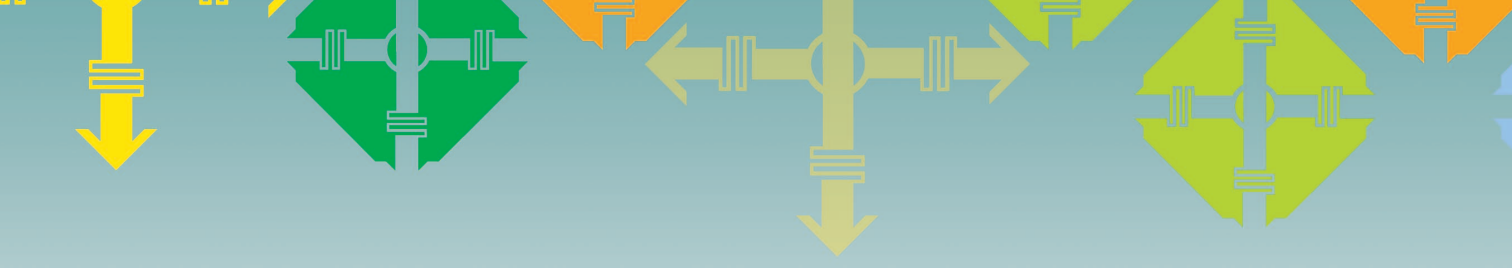
A review.

Crossed dipole antennas have been widely developed for current and future wireless communication systems. They can generate isotropic, omnidirectional, dual-polarized (DP), and circularly polarized (CP) radiation. Moreover, by incorporating a variety of primary radiation elements, they are suitable for single-band, multiband, and wideband operations. This article presents a review of the designs, characteristics, and applications of crossed dipole antennas along with the recent developments of single-feed CP configurations. The considerations of profile miniaturization, radiation pattern control, bandwidth enhancement, and multiband operation are emphasized.

Digital Object Identifier 10.1109/MAP.2015.2470680
Date of publication: 6 October 2015

THE HISTORY OF CROSSED DIPOLE ANTENNAS

The crossed dipole is a common type of modern antenna with a radio frequency (RF)-to millimeter-wave frequency range. The crossed dipole antenna has a fairly rich and interesting history that started in the 1930s. The first crossed dipole antenna was developed under the name “turnstile antenna” by Brown [1]. In the 1940s, “superturnstile” antennas [2]–[4] were developed for a broader impedance bandwidth in comparison with the original design. In 1961, a new type of crossed dipole antenna, which used a single feed, was developed for CP radiation [52]. In the 2000s, the crossed dipoles began to be fed by two separate ports with the requisite 90° phase difference between them to generate DP radiation [30]–[51]. Today, this antenna type is used in many wireless communication systems, including broadcasting



The crossed dipole is a common type of modern antenna with an RF- to millimeter-wave frequency range.

services [1]–[14], satellite communications [26]–[29], mobile communications [30]–[51], global navigation satellite systems (GNSS) [17], [68]–[71], [74]–[79], RF identification (RFID) [65], [66], [73], wireless power transmission [15], wireless local area networks (WLANs) [80], wireless personal area networks [14], and world-wide interoperability for microwave access (WiMAX) [81].

The first crossed dipole antenna was developed with an emphasis as a new ultrahigh frequency (UHF) radiating system that economized energy by concentrating it in the horizontal plane equally in all directions [1]. A single element of this turnstile antenna is the basic design of the crossed dipole, which consists of a set of two half-wavelength dipoles aligned at right angles to each other with currents of equal magnitude that are in-phase quadrature. Since then, alternative modifications of the traditional turnstile antenna have achieved a broader impedance bandwidth, profile miniaturization, and ease of manufacturing [2]–[15]. Along with the development of wireless communications, many applications require antennas that radiate a unidirectional pattern with a significant front-to-back ratio to ensure high security and efficiency in the propagation channels. Accordingly, the crossed dipole is generally equipped with a reflector to generate a desired unidirectional pattern with circular polarization [16]–[29] or dual polarization [30]–[51]. Most of the above-mentioned antennas require a dual-feed structure that generally complicates the antenna design and fabrication. Bolster [52] demonstrated theoretically and experimentally that single-feed crossed dipoles connected in parallel could generate CP radiation, if the lengths of the dipoles were such that the real parts of their input admittances were equal and the phase angles of their input admittances differed by 90° . Based on these conditions, numerous single-feed CP crossed dipole antennas [53]–[81] have been reported. With the rapid development of today's wireless communication markets, higher demands have been raised for the antenna design, including compact sizes; high efficiencies; broad bandwidths; multiple bands; specific radiation profiles; ease of fabrication and integration; and low costs. A number of alternative engineering approaches have been used to tailor the crossed dipole antenna design to address these issues.

In the eight decades since the first crossed dipole was proposed, there has been a vast amount of literature on crossed

dipole antennas. However, there is still no review article or book that discusses all types of these antennas. In this article, the design, characteristics, and applications of crossed dipole antennas are reviewed. The theoretical developments for crossed dipole antennas have been essentially completed; consequently, this review will emphasize antenna application-oriented contributions. The crossed dipole antenna types are roughly divided into four different classes based on their feeding structures and radiation characteristics.

ISOTROPIC AND OMNIDIRECTIONAL CROSSED DIPOLE ANTENNAS

Broadcasting most frequently refers to the transmission of information and entertainment programming from various sources to the general public. Commercial broadcasting began in the 1920s for audio services and in the 1950s for television. Antennas for broadcasting transmitters are usually located in the heart of a city and require radiating an equal signal in all directions in the horizontal plane. Among the antenna designs for broadcast purposes, the “turnstile” antenna was one of the first [1]. With the development of broadcasting services, different types of broadcasting antennas have been developed for broadening bandwidth, higher gain, and polarization control, as well as ease of installation. These designs are reviewed in this section.

A UHF antenna was developed in [1] with the purpose to embody the features of circularly symmetrical radiation with increased horizontal directivity into a sturdy structure, possibly supported by a single mast. The turnstile antenna was finally constructed and fulfilled these conditions. Figure 1(a) shows the basic geometry of a single turnstile antenna. It consists of a set of two half-wavelength dipoles aligned at right angles with respect to each other; the currents on the dipoles have equal magnitude and are in-phase quadrature. Consequently, the turnstile antenna is often referred to as a *crossed dipole antenna*. It has a near-isotropic radiation pattern [Figure 1(b)], i.e., it is linearly polarized with a circularly symmetrical profile in the horizontal plane (x – y plane) and CP radiation in the $\pm z$ directions; the front side radiates left-hand circular polarization (LHCP), while the back side radiates right-hand circular polarization (RHCP). A double turnstile in free space with a vertical separation of 0.25λ , as shown in Figure 2(a), generates an isotropic radiation pattern [16]. This

behavior is attributed to the two dipoles of each turnstile realizing an omnidirectional pattern in the horizontal plane, while the two turnstiles being separated by a quarter-wavelength leads to uniform radiation in the vertical plane. As shown in Figure 2(b), the double turnstile provides a broadened radiation pattern with respect to that of the single turnstile [Figure 1(b)]. Moreover, a 0-dBi gain is maintained over almost all directions in the entire three-dimensional (3-D) space. To further increase the horizontal signal strength and maintain the shape of the horizontal pattern, more elements are placed in a vertical array [1].

Based on the conventional turnstile design, several modifications, such as the pretuned turnstile [2], cloverleaf [3], and batwing [4] shapes, have been developed to produce wider impedance bandwidths. In particular, the batwing antennas yielded better performance in comparison with the others and had a broader bandwidth, lower profile, easier adjustment of matching conditions, and easier polarization control. Due to these features, batwing radiators, which are often called *superturnstile antennas*, have been installed in most broadcasting systems [4]–[9], while the other designs have been almost entirely phased out.

Figure 3(a) shows the normal configuration of the batwing radiator with four wings placed around a central metal mast. Each wing connects to the mast at its top and bottom with a metal-to-metal connector. The inner vertical rod and the sup-

port mast form a two-line slot fed by a metal jumper located at the center of each wing. The matching condition is obtained by changing the shape of the jumper and by changing the distance between the support mast and the antenna elements. To produce an omnidirectional pattern in the horizontal plane, a feed power divider located inside the mast properly phases the inputs for CP performance (0° , 90° , 180° , and 270°). A single batwing antenna normally provides a fractional bandwidth of approximately 50% and is ideally suited when low to medium gain is required. With a proper arrangement of their radiators, superturnstile antennas can be used for either horizontal [4] or vertical polarization [5].

An omnidirectional gain up to 10 dBi can be achieved with a multiple bay antenna constructed on a single modular mast [7]. For instance, as shown in Figure 3(b), a superturnstile television broadcasting antenna contains four bays mounted on a single mast. An opposing pair of wings functions as a dipole, with each pair of crossed dipoles fed 90° out of phase to create an omnidirectional radiation pattern. The vertical collinear stack of batwings increases the gain of the antenna, concentrating the radiation in the horizontal direction, so that only a little power is radiated toward the sky or the ground. Two or more elements, each covering a different frequency band, have been mounted on a single mast to effectively span a much wider range of frequencies. By combining the horizontally polarized and the vertically

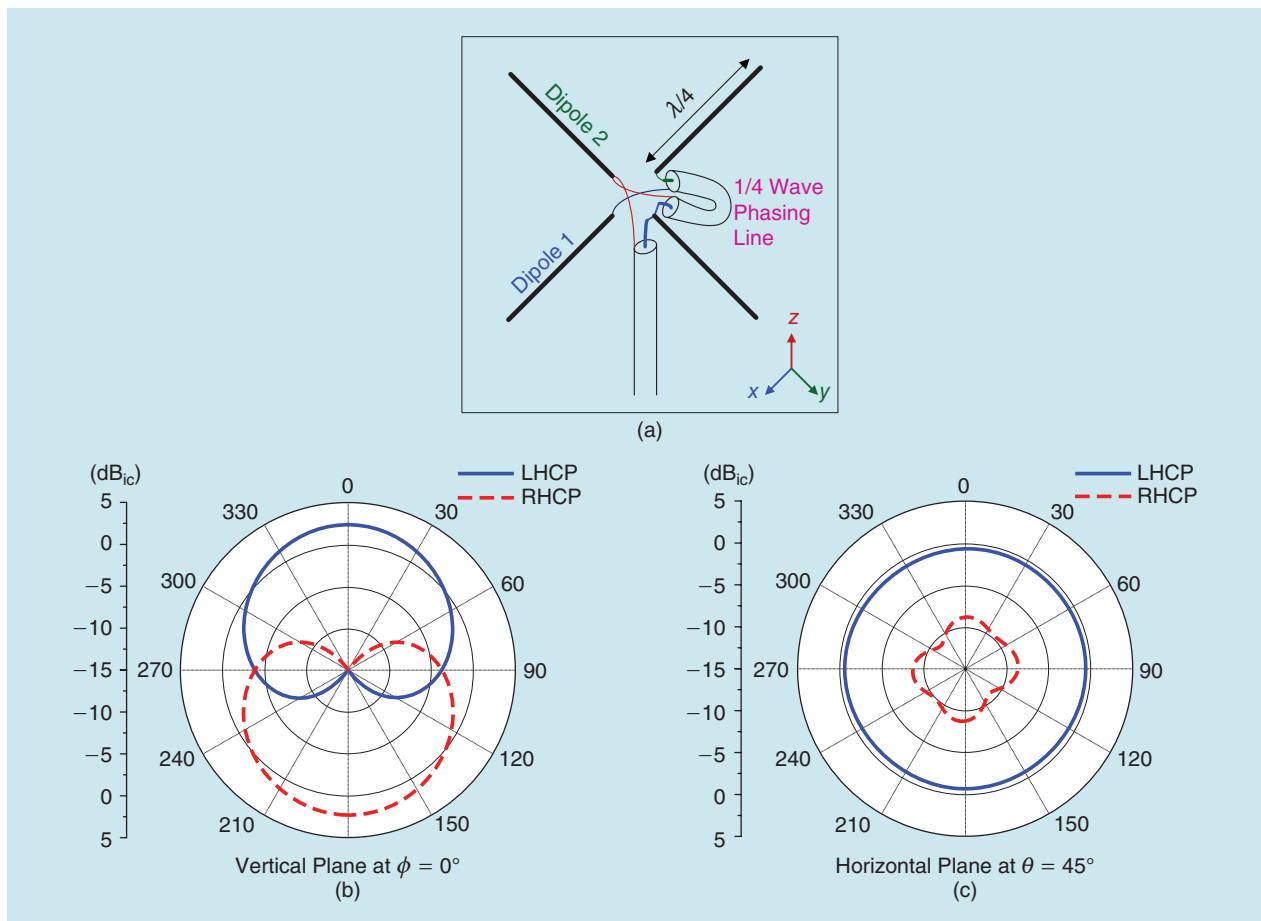


FIGURE 1. A turnstile antenna. (a) The 3-D view and (b) its vertical-plane pattern (c) and horizontal-plane pattern at the resonant frequency [1].

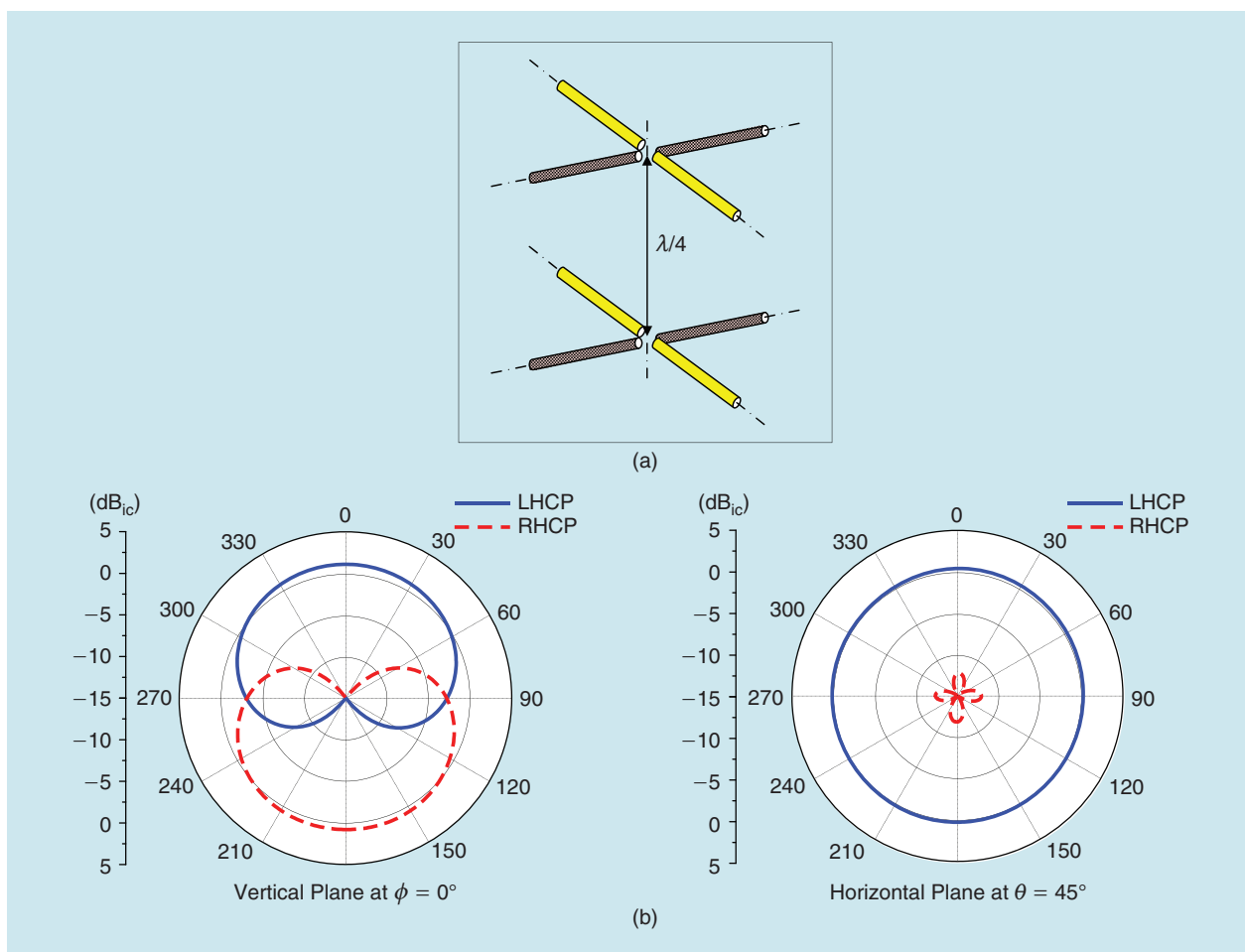


FIGURE 2. A double-turnstile antenna in free space. (a) The 3-D view and (b) its radiation pattern at the resonant frequency [16].

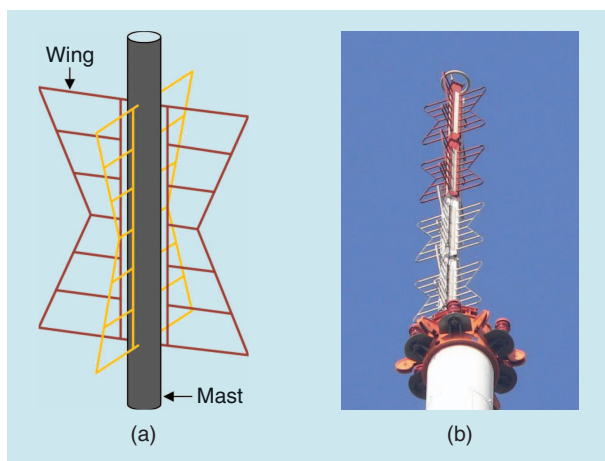


FIGURE 3. A batwing antenna. (a) The normal configuration [4] and (b) a superturnstile television broadcasting antenna at the Muehlacker television transmitter, Muehlacker, Germany. [Source: Figure 3(b) is from Wikipedia, the free encyclopedia. https://en.wikipedia.org/wiki/Batwing_antenna.]

polarized batwing antennas, a CP omnidirectional antenna was constructed for high-power broadcasting transmitters [8]–[11]. Recently, several types of modified batwing antennas [12] have

been developed to enhance the performance in impedance bandwidth, gain, and profile miniaturization. These antennas employed an unbalanced feed-line type and a parallel coupling type for better performance.

Each turnstile element generally requires a dual feed or a sequentially rotated feed, and consequently, the feeding network of a superturnstile with multibays requires several phase delay lines and power combiner/splitters. Cost and the difficulty of manufacturing the feeding structures are the main challenges of antenna designs for broadcasting transmitters. To reduce the cost of construction, antennas for different systems are generally mounted on a single mast. Therefore, the mutual coupling between the antennas needs to be considered. In addition, some new types of turnstile antennas have been considered to produce an isotropic radiation pattern with a single feed [13], [14], or CP radiation with an electrically small size [15].

UNIDIRECTIONAL CIRCULARLY POLARIZED CROSSED DIPOLE ANTENNAS

As noted, a conventional crossed dipole [Figure 1(a)] is used to produce CP radiation in the $\pm z$ direction. To generate unidirectional CP radiation, the crossed dipoles are generally placed on a perfect electric conductor (PEC) reflector, as

shown in Figure 4. The presence of the PEC surface redirects one-half of the radiation into the opposite direction, improving the antenna gain by approximately 3 dB and partially shielding objects on the other side. This is observed in Figure 5, which shows the 3-D radiation patterns of the ideal crossed dipole [16] at its resonance in free space and above a finite square PEC surface. This antenna has a resonant frequency of 3 GHz and was characterized by using the ANSYS-Ansoft high-frequency structure simulator (HFSS). In free space, the crossed dipole radiates a quasi-isotropic radiation pattern with a maximum gain of 2.5 dBi and a minimum gain of -2 dBi [Figure 5(a)]. For the PEC reflector case with the distance of separation between the antennas and the ground plane being $H = 0.25 \lambda$, the antenna radiates a broadside radiation pattern with a gain of 7.7 dBi and a front-to-back ratio of 13 dB. If the antenna is too close to the PEC surface, the image currents cancel the currents in the antenna, resulting in poor radiation efficiency. This problem is addressed typically by including a quarter-wavelength space between the radiating elements and the reflector for optimal antenna characteristics. For profile miniaturization, the crossed dipole can be backed by an artificial magnetic conductor (AMC) surface [17]. The AMC surface provides the desired broadside radiation pattern and allows the placement of the antenna in close proximity to it with good impedance matching. The characteristics of the crossed dipole on an AMC surface will be discussed in the next section.

Several other combinations have been considered to achieve unidirectional radiation patterns. For instance, a log-periodic crossed dipole antenna [18], [19] and a Yagi-Uda turnstile antenna [20] were successfully constructed and tested. These antennas have been widely applied to satellite communications [16], GNSS [17], electromagnetic interference measurements [18], and coherent electromagnetic radio tomography [20].

For broadband applications, the straight half-wavelength dipole is generally replaced by modified radiators that have wider bandwidth responses [21]–[29]. These designs also require a wideband dual feed that delivers equal amplitudes to the radiators with a 90° phase difference between them to generate the desired CP radiation. Excitation can be accomplished by employing a feeding network, such as a turnstile network [22], Wilkinson power divider [24], microstrip line to double-slot line transmission [25], T-junction power divider [26]–[28], or Wilkinson power divider with two stubs [29]. Most of these structures generally contain a 1-to-2 power combiner/splitter and quarter-wavelength phasing.

Antennas for some applications need to have specific radiation characteristics, e.g., specific directivity, beamwidth, and front-to-back ratio values. For instance, the antenna for television broadcast services [21] is required to have a half-power beamwidth (HPBW) of 120° and 90° in three and four element array configurations, respectively. However, the radiation patterns of a crossed dipole antenna equipped with a planar PEC reflector are normally insufficient to meet these requirements.

To circumvent this problem, several techniques have been employed to improve their radiation characteristics, including gain, front-to-back ratio, beamwidths, and axial ratio (AR). The

integration of a cavity-backed reflector with the crossed dipole antenna is a popular technique that achieves a unidirectional behavior while providing higher gain and easy pattern control. As an example, Figure 6 shows the geometry of a wideband, high-gain antenna that is a composite cavity-backed crossed bowtie system [25]. The antenna yielded an impedance matching bandwidth of over 57% with a voltage standing wave ratio (VSWR) < 2 , a 3-dB AR bandwidth of 39%, a broadside gain of 8–10.7 dBi, and a symmetrical radiation pattern over the entire operating-bandwidth range. Other techniques, such as a shorted bowtie [24], droopy dipole [22], [23], narrow patch connection [28], and vertical top-hat [29], have been implemented as the primary radiation elements to achieve a wider 3-dB AR beamwidth and a higher gain. These broadband CP crossed dipole antennas have been widely applied to television broadcast services, global positioning systems (GPS), and International Maritime Satellite Organization communications.

Similar to the antennas described in the “Isotropic and Omnidirectional Crossed Dipole Antennas” section, the dual feed of these crossed dipole antennas requires equal magnitude and a 90° phase difference, which complicates the antenna’s design and manufacture. Single-feed CP crossed dipole antennas

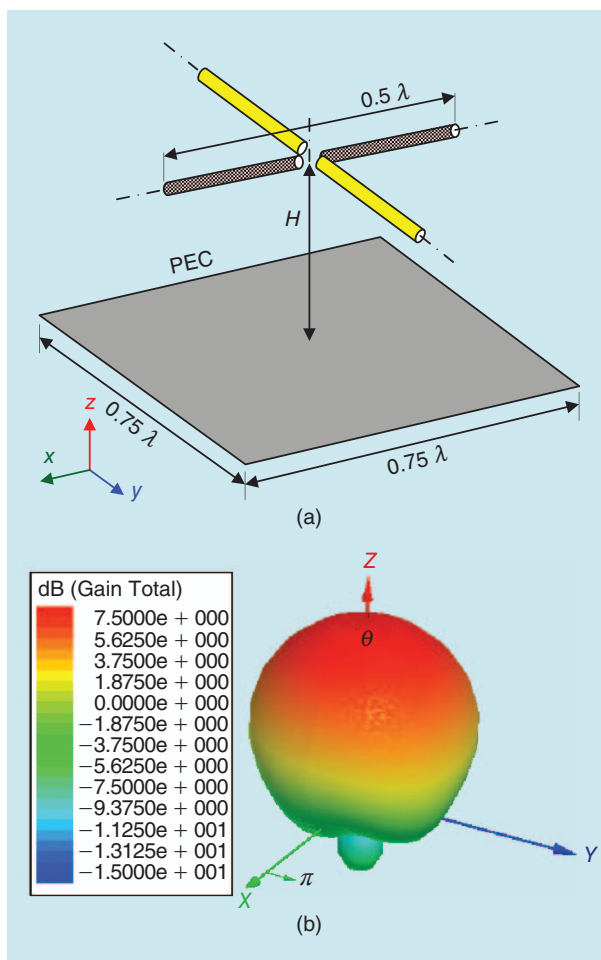


FIGURE 4. (a) A crossed dipole antenna above a finite square PEC surface. (b) The 3-D radiation pattern at the resonant frequency [16].

were developed in an effort to solve this problem. These antennas will be discussed in the “Single-Feed Circularly Polarized Crossed Dipoles” section. Nonetheless, the considerations of miniaturization, wideband operation, multiband operation, as well as the radiation pattern control, will continue to be investigated for these types of antennas. In particular, the dual-feed crossed dipole antennas on AMC (e.g., [17]), which exhibit promising characteristics of low-profile and broad bandwidth, could be an important direction for future research.

DP CROSSED DIPOLE ANTENNAS

With the development of mobile communication systems, DP antennas have been widely used to combat multipath fading and to improve the overall communication capabilities and quality. Compared with space diversity approaches, the DP antenna is able to reduce the installation space in a base station. Nevertheless, the ideal base station antenna should have broadband performance, high isolation, high front-to-back ratio, low cost, easy assembly, and the required appropriate beamwidth for the cell sector design. The basic crossed dipole antenna is easily modified to meet these requirements for a base station antenna.

To generate DP radiation, the two antennas are fed by two separate ports with the requisite 90° phase difference between them. Broadband performance is achieved by using pairs of wideband radiators. Examples include folded dipoles [30], [31], fractal-like elements [32], magnetoelectric dipoles [33]–[36],

modified bowties [37]–[49], and square-loop shape arm dipoles [50], [51]. These antennas are normally integrated with planar metallic reflectors to achieve a high front-to-back ratio. The reflector shape is engineered to create the radiation patterns that will satisfy the design requirements. Different feeding structures, including Γ -shape [34], dielectric loading [35], differentially driven [36], integrated balun [38], and shorting metal posts [41], have been used for high isolation between the two ports. These various DP crossed dipole antenna designs have also accomplished other system goals, such as low profile, bandwidth improvement, and radiation pattern control.

As shown in Figure 7, the broadband DP antenna proposed in [51] is composed of a radiator, a dielectric post, and a metallic reflector. The radiator consists of two orthogonally oriented dipoles that have square-loop-shaped arms. The antenna is excited by two Γ -shaped feeds that are embedded inside the dielectric post. The shape of the metallic reflector is engineered to control different aspects of the patterns, such as the beamwidth, cross polarization, radiation stability, and front-to-back ratio. The prototype reported in [51] has an impedance bandwidth of more than 57% with a VSWR <1.5 and a port-to-port isolation >31 dB. The peak gain of the antenna is about 8.8 dBi and varies only by ± 0.3 dBi across the working frequency range. The antenna can be used as the elements in an array that is employed in base stations for wireless communications.

Most of the older DP crossed dipole antennas are equipped with metallic reflectors. As a result, their profiles are relatively large. To achieve a low profile, the metallic reflectors can be replaced by a high impedance surface (HIS) [49]. However, the design of HIS-based DP antennas faces a key challenge: improving the bandwidth for the HIS structure. Many wireless communication systems use multiple frequency bands simultaneously. Consequently, multiband DP antennas (e.g., [47]) need further consideration.

SINGLE-FEED CIRCULARLY POLARIZED CROSSED DIPOLES

As mentioned previously, a straightforward way to generate CP radiation is to utilize two orthogonally crossed dipoles excited by

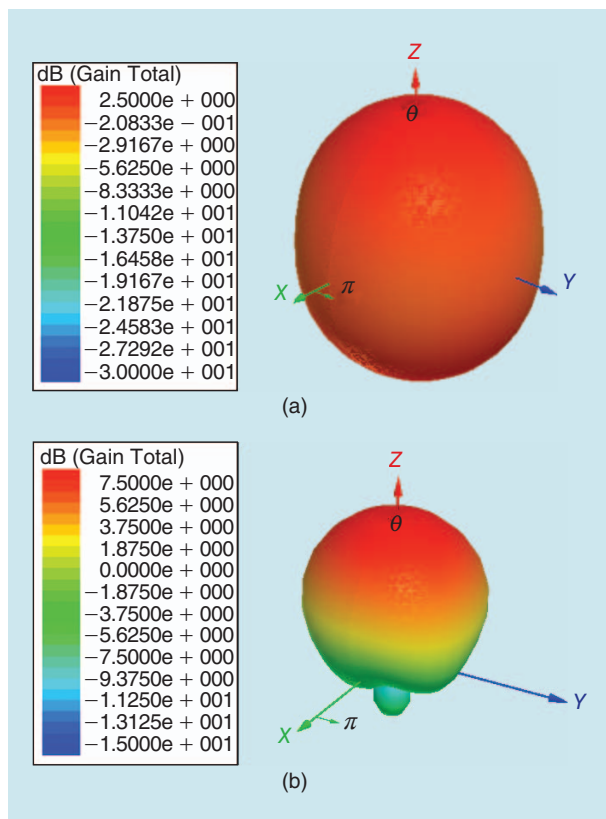


FIGURE 5. The 3-D radiation patterns of the turnstile antenna at its resonance for different configurations: (a) in free space and (b) above a finite square PEC surface.

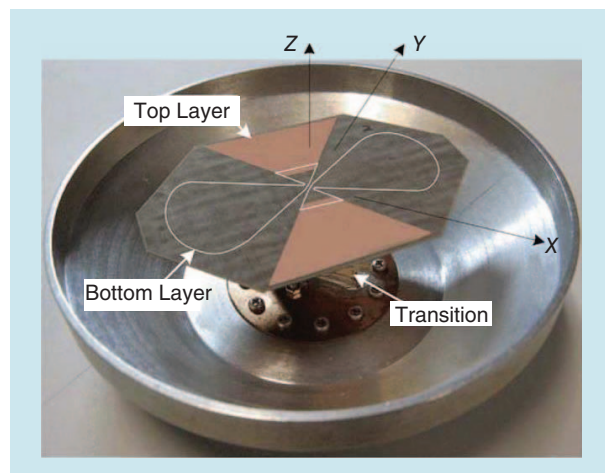


FIGURE 6. A crossed bowtie dipole antenna backed by a cavity [25].

two sources with equal magnitude and a 90° phase difference. The excitation can be accomplished by a feeding network with a 1-to-2 power combiner/splitter and a quarter-wavelength phase shifter. This approach is attractive for a broadband CP antenna, but generally complicates the antenna design and fabrication. Another method to obtain a CP wave was shown in [52]. It uses two orthogonal dipoles excited in parallel by a common generator, but without any matching network. The required power and phase relationships are obtained by properly choosing the lengths of the two dipoles. Based on this approach, a variety of single-feed CP crossed dipole antennas have been developed for different applications. Recent developments with these designs are examined in this section.

CONDITIONS FOR CP RADIATION

The conditions to obtain CP radiation from two orthogonal dipoles with a single feed were detailed in [52]. These conditions are reviewed briefly here. Figure 8(a) shows the two orthogonal cylindrical dipoles fed in parallel and a representative equivalent circuit. Assume that their lengths are much greater than their radii and that each dipole is placed in the neutral (or zero) potential plane of the other dipole to establish negligible mutual coupling between the two dipoles. To generate a CP wave, the antenna must have equal power input to each dipole and a 90° phase difference between their input currents. This is equivalent to having

$$G_X = G_Y \quad \text{and} \quad \arg \bar{Y}_X = \arg \bar{Y}_Y \pm 90^\circ, \quad (1)$$

$$\bar{Y}_X = G_X + jB_X \quad \text{and} \quad \bar{Y}_Y = G_Y + jB_Y, \quad (2)$$

where \bar{Y}_X and \bar{Y}_Y are the admittances of the dipoles in the x and y directions, respectively. G_X and G_Y are the conductances (the real part) and B_X and B_Y are the susceptances (the imaginary part) of the admittances of the dipoles in the x and y directions, respectively. The dipole admittance depends on its length. The input admittance of a cylindrical dipole with a radius of $0.002 \lambda_0$ as a function of its length was calculated in free space with the HFSS software and is given in Figure 8(b). The condition for CP radiation can be determined from an accurate plot of the dipole admittance by a graphical solution, as shown in Figure 8(b), i.e., the antenna radiates CP radiation with h_x and h_y approximately equal to $0.51\lambda_0$ and $0.42\lambda_0$, respectively. At the desired frequency, the longer one has an inductive reactance while the shorter one has a capacitive reactance. This approach for CP wave generation has been experimentally demonstrated in [53]. As shown in Figure 9, a crossed dipole was designed and constructed at 1.7 GHz ($\lambda_0 \sim 176$ mm). The antenna included two dipoles with lengths of 93 ($\sim 0.527\lambda_0$) and 74 mm ($\sim 0.42\lambda_0$). The prototype was constructed using 2.1-mm-diameter, semirigid, coaxial cable with an subminiature version A (SMA) connector at the input port to feed the orthogonal wire arms of the dipole. A folded balun consisting of a $0.25\lambda_0$ (44 mm) conductor was soldered between the two orthogonal dipole arms that connect with the center conductor of the coax and the cable sheath. The measurements yielded two resonances (one

<1.7 GHz and the other >1.7 GHz) in the return loss profile and a boresight cross-polar level of approximately -14 dB ($AR = 3.5$ dB) at 1.7 GHz. Based on this condition, many single-feed crossed unequal-length dipoles [54]–[59] and other types of antennas, such as wideband dipoles [60]–[62], slot antennas [63], [64], meander-line dipoles [65], [66], [72]–[81], and near-field resonant parasitic (NFRP) antennas [67]–[71], have

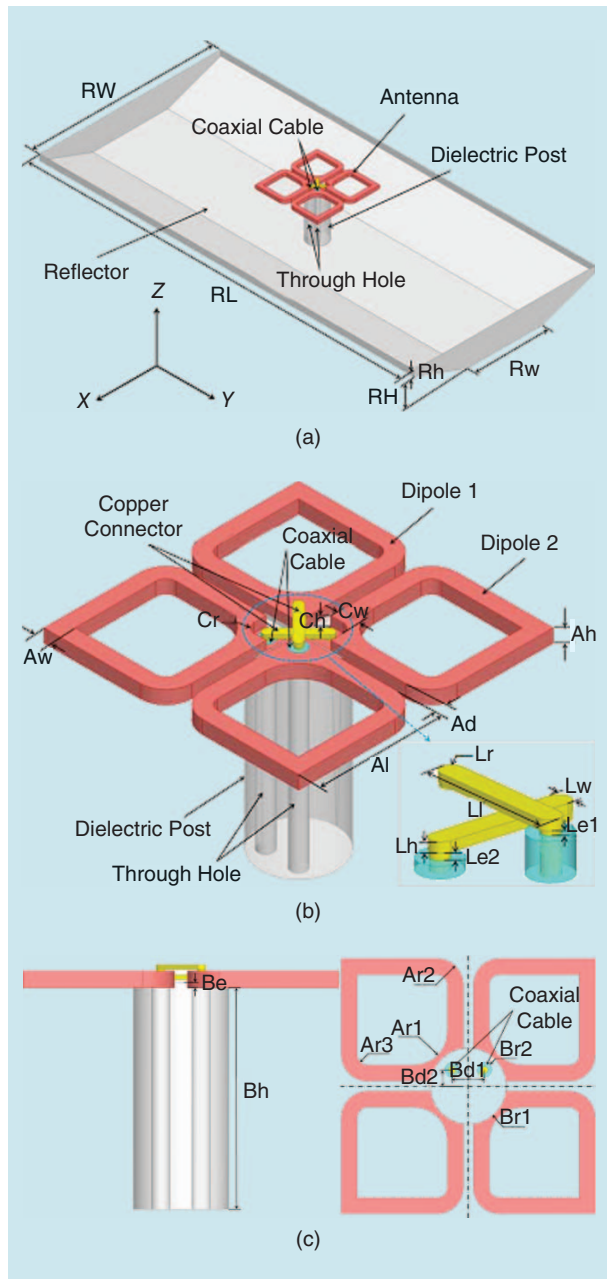


FIGURE 7. The configuration of a broadband DP crossed dipole antenna. (a) The overall diagram of the antenna system including its reflector. (b) The crossed dipole. (c) The side and bottom views [51]. RL = 300, RW = 145, Rr = 60, RH = 15.5, Rh = 4.5, Al = 23.8, Aw = 3.0, Ah = 2.6, Ad = 2.1, Ar1 = 6.0, Ar2 = 5.0, Ar3 = 2.0, Cw = 4.2, Ch = 1.8, Cr = 1.8, Ll = 10.4, Lw = 2, Lr = 1.6, Lh = 0.7, Le1 = 0.3, Le2 = 0.5, Bh = 34.7, Be = 0.8, Br1 = 7.5, Br2 = 1.5, Bd1 = 2, and Bd2 = 6.4 (units: mm).

been constructed for CP radiation. These various designs are reviewed in the following sections.

CP NFRP ANTENNAS

The NFRP antenna is a type of metamaterial (MTM)-inspired antenna [67] that is constructed from a single MTM unit cell to achieve the desired matching and a high radiation efficiency. To achieve CP radiation, two inductive-based (capacitive-based) NFRP elements placed in an effective crossed dipole configuration need to generate two resonances, i.e., one that is tuned to be below the desired operating frequency, creating an inductive (capacitive) reactance, the other is tuned to be resonant above the desired operating frequency, creating a capacitive (an inductance) reactance. A GPS L1 CP antenna, shown in Figure 10, has been obtained [68] using two capacitively loaded loop-based wire NFRP elements; it is fed by a coaxial semi-loop antenna. The requisite phase shift is obtained by tuning the angle between the semi-loop antenna and the NFRP elements. It has a 30.7-MHz bandwidth for $|S_{11}| < -10$ dB and a 7.9-MHz bandwidth for the 3-dB AR. At 1,575.4 MHz, the antenna yields an overall efficiency of 96.9%, a broadside gain of 6.28 dBi, and an AR of 0.6 dB. The CP radiation condition has also been achieved with the protractor antenna NFRP

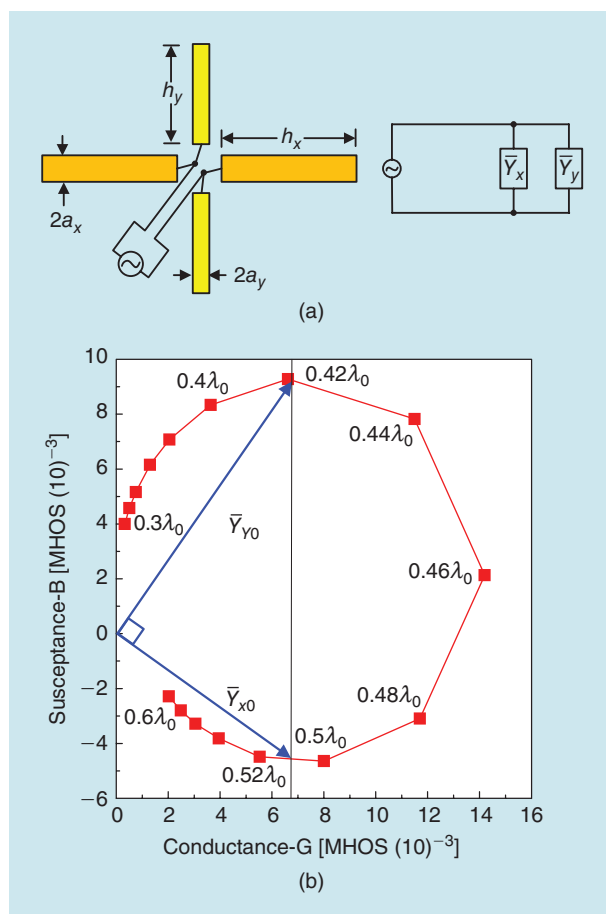


FIGURE 8. The two orthogonal cylindrical dipoles fed in parallel. (a) The arrangement of the dipoles and its equivalent circuit [52]. (b) The input admittance of a single dipole as a function of its length.

structure [69] shown in Figure 11. Each protractor element produces a magnetic dipole parallel to the ground plane. At the desired frequency, one was designed to create an inductive reactance while the other was designed to create a capacitive reactance. The optimal design with a height of 15 mm yielded 29.3 MHz for $|S_{11}| < -10$ dB, 7.2 MHz for 3-dB AR, 89.2% overall efficiency, and AR = 0.26 dB at the GPS L1 frequency. A dual-band CP NFRP antenna for the GPS L1/L2 bands [69] has been achieved by using two orthogonal dual-band protractor elements whose design is shown in Figure 12(a) and whose fabricated prototype is shown in Figure 12(b). Two pairs of protractor NFRP elements were designed to have the appropriate phasing between their resonances to produce the CP radiation at both the GPS L1 and L2 frequencies with a single-feed structure. The final design with a height of 19.4 mm was constructed on a 119.5-mm-diameter ground plane. The antenna has an $|S_{11}| < -10$ -dB bandwidth of 10.6 and 24.2 MHz, and a 3-dB AR bandwidth of 4.3 and 5.3 MHz for the GPS L1 and L2 bands, respectively. At the GPS L1 frequency, it has an overall efficiency of 79.2%, a gain of 6.2 dBi, and an AR of 0.87 dB. At the GPS L2 frequency, it has an overall efficiency of 71.1%, a gain of 5.36 dBi, and an AR of 0.42 dB.

To further improve the low-profile characteristics of the CP NFRP antenna, meander lines have been applied to the NFRP elements. In [70], a dual-band LP antenna with two orthogonal NFRP dipoles was first designed for GPS L1 and Global Star applications, and then the two dipoles

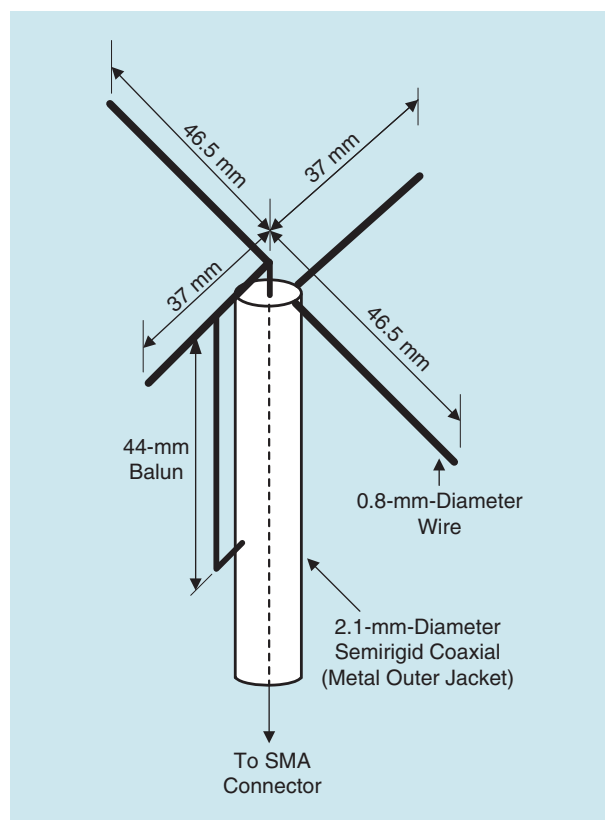


FIGURE 9. The layout of a prototype 1.7-GHz CP dipole [53]. SMA: subminiature version A.

were retuned to have overlapping resonances that exhibit a 90° phase difference between them at the GPS L1 frequency for CP radiation. Figure 13 shows the geometry of the GPS L1 CP NFRP antenna; it is a planar structure with a very small size of $25.4 \text{ mm} \times 25.4 \text{ mm}$ ($\lambda_o/7.5 \times \lambda_o/7.5$ at 1.5754 GHz). The antenna is built on Rogers Duroid 4350 substrate with a relative permittivity of 3.66, a loss tangent of 0.004, and a thickness of 0.762 mm. The final design has an $|S_{11}| < -10$ -dB bandwidth of approximately 70 MHz, a 3-dB AR bandwidth of approximately 17 MHz, and a minimum AR at 1.580 GHz with a value of 0.84 dB. At this frequency, the antenna radiated a quasi-isotropic radiation pattern with a peak directivity of 1.88 dBi and an overall efficiency of 73.41%. To achieve a unidirectional radiation pattern with a low profile, another CP NFRP antenna, shown in Figure 14, has been equipped with an AMC surface [71]. Its main radiating element consists of two slightly different-sized, orthogonally oriented, and Egyptian axe NFRP elements. The driven element

also consists of two slightly different-sized, orthogonally oriented, top-loaded dipoles that are coaxially fed. The antenna was built on Rogers Duroid 5880 substrate with a relative permittivity of 2.2, a loss tangent of 0.0009, and a thickness of 0.7874 mm. The AMC structure was implemented on a Trans-Tech MCT-40 ceramic material with a relative permittivity of 40, a loss tangent of 0.0015, and a thickness of 5 mm. The final design with a 60-mm-diameter footprint and a total height of 8.7874 mm has an impedance matching bandwidth of 1.5586–1.6071 GHz (48.5 MHz) for $|S_{11}| < -10$ dB and a 3-dB AR bandwidth of 1.5696–1.5812 GHz (11.6 MHz). At the GPS L1 frequency, the AR is 0.2548 dB, the overall efficiency is 79.6%, and the maximum gain is 4.25 dBi along the broadside direction.

The NFRP antennas have yielded small electrical size, good impedance matching, good CP radiation, and high radiation efficiency. However, these antennas suffer from narrow bandwidths. In addition, their configurations are too complicated to implement for multiband operation. Multiband CP antennas using planar NFRP elements would be yet another interesting direction to address the aforementioned issues.

MULTIBAND WIDEBEAM CP CROSSED DIPOLE ANTENNAS

The GPS satellites conventionally operate in two frequency bands at the same time, i.e., L1 (1.57542 GHz) and L2 (1.2276 GHz). Recently, several bands, namely, the GPS L3 (1.38105 GHz), L4 (1.379913 GHz), and L5 (1.17645 GHz), have been added for special applications (e.g., nuclear detonation detection, additional ionospheric correction, and civilian safety-of-life signal reception). In addition, the GPS receiver antenna requires a CP beamwidth of 100° – 140° for terrestrial and 120° – 160° for airborne applications. By properly combining compact multiresonant dipoles and a cavity-backed reflector, multiband widebeam CP crossed dipole antennas have been realized for use in GPS receivers.

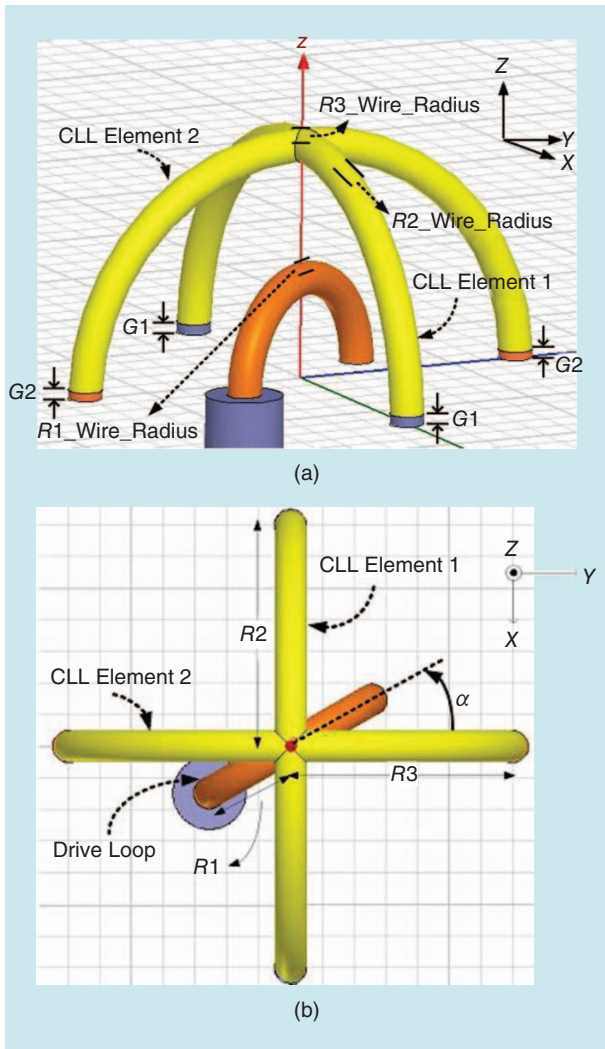


FIGURE 10. A GPS L1 CP NFRP wire antenna [68]. (a) The 3-D view. (b) The top view. $R1 = 5.9 \text{ mm}$, $R1_wire_radius = 1.0 \text{ mm}$, $R2 = R3 = 14.0 \text{ mm}$, $R2_wire_radius = R3_wire_radius = 1.0 \text{ mm}$, $G1 = 0.193 \text{ mm}$, $G2 = 0.182 \text{ mm}$, and $\alpha = 30^\circ$.

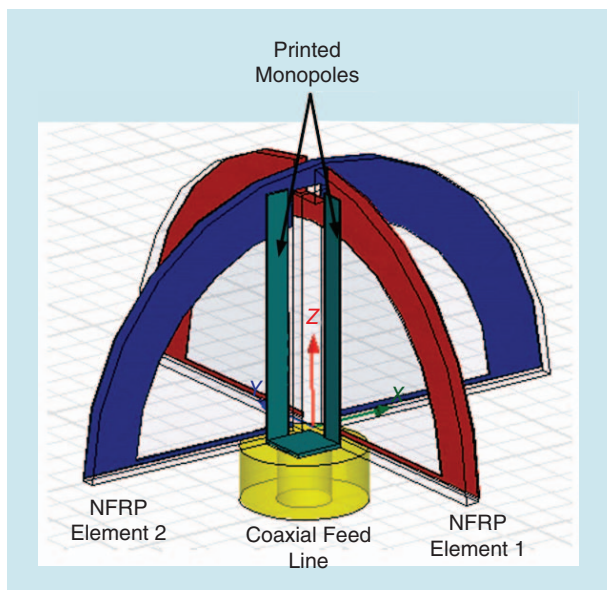


FIGURE 11. The 3-D view of a GPS L1 CP antenna with two orthogonally oriented NFRP elements [69].

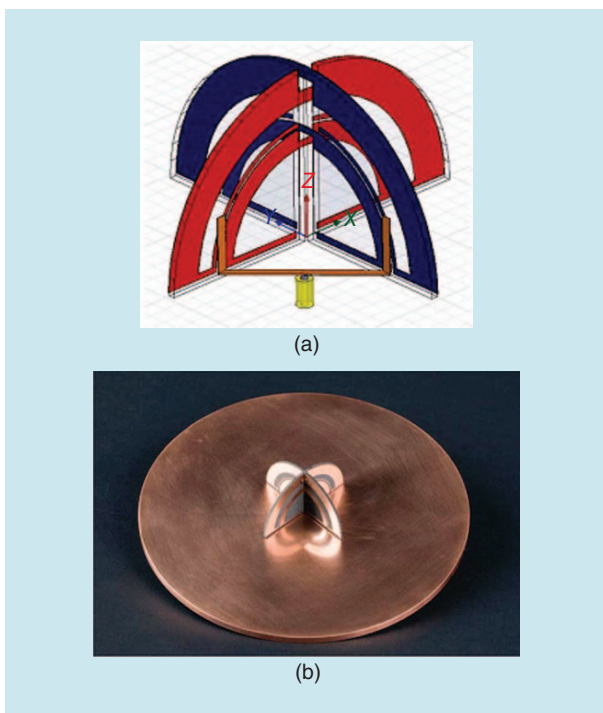


FIGURE 12. The dual-band CP NFRP antenna for GPS L1/L2 bands. (a) The design of the primary radiation elements. (b) A fabricated prototype [69].

Two techniques, namely, the insertion of a meander line in the dipole arm and an arrowhead-shaped trace at its end, were used to achieve a compact size [70], [72]. The process of the dipole length reduction is illustrated in Figure 15. The initial design was a half-wavelength dipole (0.5λ). To reduce its length, but keep the same resonance, two meander lines were symmetrically inserted into the arms of the initial design. To further reduce its length, the ends of the dipole were formed into a barbed shape. The final design has a much shorter length (0.3λ) and the same resonance in comparison with the initial dipole. However, the length reduction was accompanied by a degradation of the antenna characteristics such as the impedance matching bandwidth. Therefore, the design parameters of the dipole chosen were a compromise between compactness and broadband characteristics. The meander-line dipoles are incorporated with a pair of vacant-quarter printed rings to construct a compact radiator with a good impedance matching and good CP radiation. This compact crossed dipole can be used as single element radiator [73] or can be equipped with a cavity-backed reflector to produce a unidirectional radiation pattern with a wide 3-dB AR beamwidth and a high front-to-back ratio [74], [75].

To add another resonance, dipole number three in Figure 15 was modified by creating an asymmetrically barbed arrowhead, as shown in Figure 16(a). This design, denoted as dipole number four, contains two meander lines and two half-arrowheads of different sizes. Dipole number four was designed to have two resonances near 1.227 and 1.575 GHz, as shown in Figure 16(b). To achieve CP radiation at both the GPS L1/L2 bands, dipole number four is crossed through a

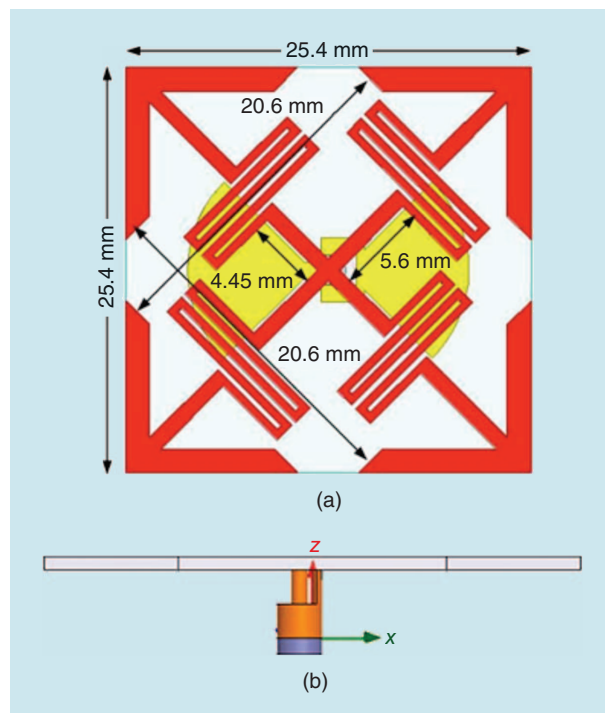


FIGURE 13. A CP NFRP antenna for the GPS L1 band. (a) The top view. (b) The side view [70].

double vacant-quarter printed ring [Figure 17(a)]. By properly adjusting the ring and dipole number four, the appropriate phasing between the resonances to produce CP radiation is obtained at both of the desired frequencies. The cavity-backed reflector was also used to improve the radiation patterns of the crossed asymmetric dipole antenna [76]. Figure 17(b) shows a cross-sectional view of the prototype antenna. Thanks to the presence of the cavity, the 3-dB AR beamwidth was significantly widened at both bands. The final design of the GPS L1/L2 antenna with an overall size of $120\text{ mm} \times 120\text{ mm} \times 40.5\text{ mm}$ has an impedance matching bandwidth of 1.188–1.265 GHz (48 MHz) and 1.453–1.80 GHz (347 MHz) for $|S_{11}| < -10\text{ dB}$ and a 3-dB AR bandwidth of 1.217–1.240 GHz (23 MHz) and 1.525–1.630 GHz (105 MHz), respectively. At the GPS L1 frequency, the antenna has a gain of 7.5 dBic, a radiation efficiency of 97.4%, and a 3-dB AR beamwidth of 143° and 152° in the x - z and y - z planes, respectively. At the GPS L2 frequency, the antenna has a gain of 6.3 dBic, a radiation efficiency of 90%, and a 3-dB AR beamwidth of 132° and 140° in the x - z and y - z planes, respectively. The 3-dB beamwidth can be further improved by a modification in the asymmetric dipole. This has been demonstrated in [77], which presents a dual-band crossed scythe-shaped dipole antenna with a CP radiation beamwidth $>160^\circ$ in both bands.

For multiband operation, two other branches with different lengths are added to the arm of dipole number four design in Figure 16(a). Thus, the design is referred to as a multibranch dipole, as shown in Figure 18(a). It was possible to combine the multiband dipoles and double vacant-quarter printed ring

with appropriate phasing between the resonances to produce CP radiation at the GPS L1–L5 frequencies with a single feed [78]. As shown in Figure 18(b), the crossed multibranch dipoles are backed by an inverted pyramidal cavity with a rectangular bottom measuring 120 mm \times 120 mm, a top aperture measuring 160 mm \times 160 mm, and a height of 40 mm to achieve widebeam radiation, a high front-to-back ratio, and a similar gain at all bands. A fabricated prototype of the CP GPS L1–L5 crossed dipole antenna is shown in Figure 18(c). The antenna has measured bandwidths of 1.131–1.312 GHz (181 MHz), 1.369–1.421 GHz (52 MHz), and 1.543–1.610 GHz (67 MHz) for impedance matching with $|S_{11}| < -10$ dB and 1.165–1.190 GHz (25 MHz), 1.195–1.240 GHz (45 MHz), 1.370–1.395 GHz (25 MHz), and 1.565–1.585 GHz (20 MHz) for an AR of <3 dB. In addition, the antenna has a wide beamwidth ($>90^\circ$ for the HPBW and $>110^\circ$ for the 3-dB AR beamwidth), high radiation efficiency ($>85\%$), and a high front-to-back ratio (>18 dB).

The compact crossed dipole antenna equipped with a cavity-backed reflector produces a unidirectional radiation pattern with a wide 3-dB AR beamwidth and a high front-to-back ratio. Due to the miniaturization of the radiator and the widebeam CP radiation, these antennas are suitable for single band or multiband applications with a bandwidth of $<10\%$. Recently, the wideband CP crossed dipole antennas with a single feed [58], [62] have received much attention. A challenge for particular consideration is the improvement of the 3-dB AR bandwidth while maintaining the widebeam CP radiation. In addition, the single-feed crossed dipoles may be a good choice of radiators in Fabry–Perot cavity antennas to achieve broadband high-gain CP radiation performance.

PROFILE MINIATURIZATION AND 3-DB AR BANDWIDTH ENHANCEMENT OF A CP CROSSED DIPOLE ANTENNA USING A FINITE AMC SURFACE

As noted previously, the main problem of an antenna equipped with a metallic reflector is often addressed by including a quarter-wavelength space between the radiating elements and the reflector to obtain optimal antenna characteristics. This can be circumvented by using an AMC surface instead of a metallic reflector. The AMC, which generally consists of a lattice of metal plates on a grounded dielectric substrate with/without grounding vias, can mimic a perfect magnetic conductor (PMC) over a certain frequency band. Consequently, the AMC allows close placement of the antenna with good impedance matching and the desired unidirectional radiation pattern. By combining the crossed dipole radiators and the finite AMC surfaces, low-profile multiband CP antennas that are nearly completely matched to a single 50- Ω source and have high radiation efficiencies have been implemented. More interestingly, surface waves propagating on the finite AMC are excited to generate extra operating bands for the radiating system. It was shown that the extra bands can be favorably used to enhance the bandwidth of the antenna. These various designs are reviewed in this section.

A new way of designing a dual-band CP antenna by integrating a single-band CP radiator with a finite AMC surface was presented in [79]. The dual-band operation was obtained

by utilizing the original band of the radiator and the first extra band caused by the surface waves propagating on the finite AMC reflector. The dual-band antenna configuration is shown

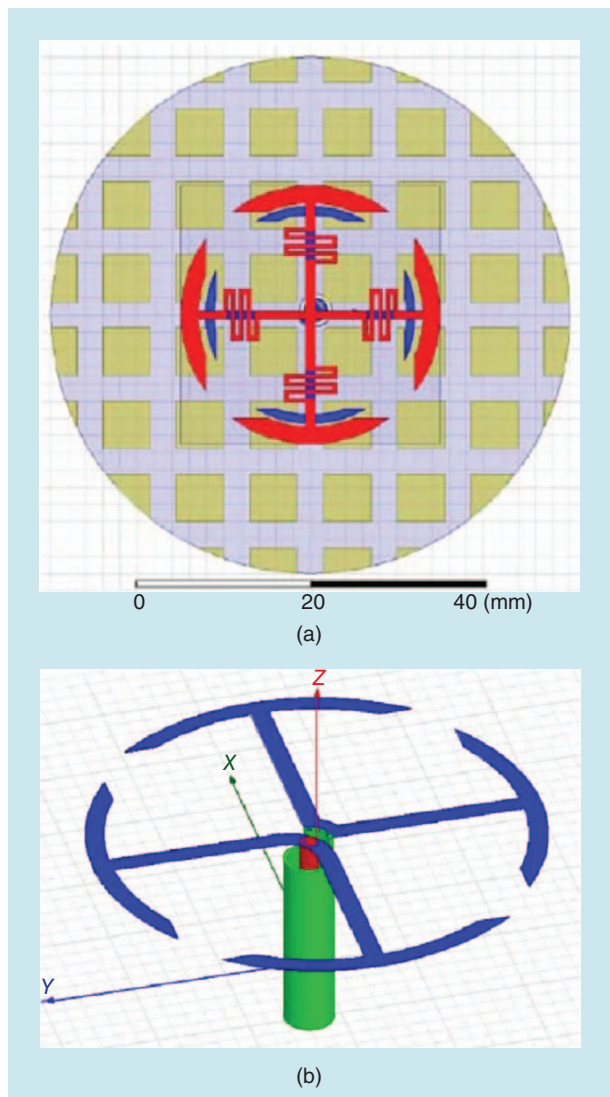


FIGURE 14. The low-profile, electrically small, high-directivity CP GPS L1 antenna. (a) The top and (b) isometric views of its driven element, which consists of two orthogonal dipoles with a single coaxial feed [71].

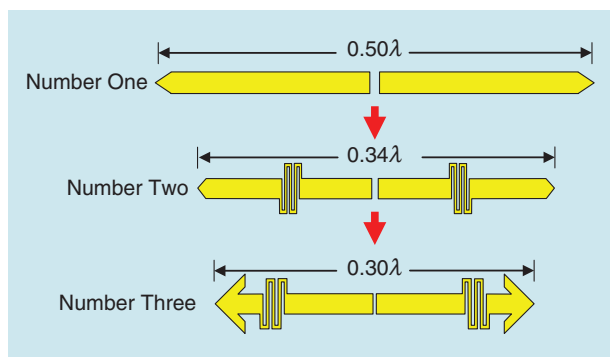


FIGURE 15. The design variations for length reduction [72].

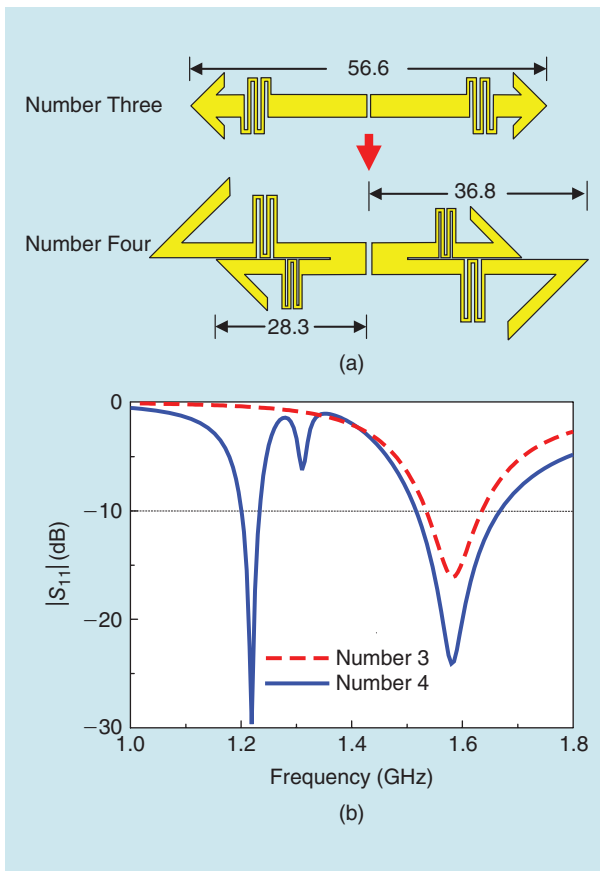


FIGURE 16. The dual-frequency generation. (a) Basic designs (dimensions in millimeters) and (b) their $|S_{11}|$ values as a function of the frequency [72].

in Figure 19. It consists of a compact crossed dipole above a 5×5 AMC surface. The antenna was optimized for the GPS L1/L2 bands with low-profile broadband characteristics and excellent CP radiation. The final design with an overall size of $85 \times 85 \times 11.493 \text{ mm}^3$ ($\sim 0.3485\lambda_o \times 0.3485\lambda_o \times 0.0471\lambda_o$ at 1.23 GHz) yields a measured impedance bandwidth of 1.202–1.706 GHz (504 MHz) for the $|S_{11}| < -10 \text{ dB}$ and 3-dB AR bandwidths of 1.205–1.240 GHz (35 MHz) and 1.530–1.625 GHz (95 MHz), respectively. The proposed antenna was RHCP in both bands and yielded gains of 5.60 and 5.31 dBi and radiation efficiencies of 95% and 96.5% at the GPS L1/L2 frequencies, respectively. Based on the proposed design method, the antenna volume can be significantly decreased by using high-permittivity materials (ϵ_{AMC}) for the AMC substrate. This was also demonstrated in [79] with a dual-band design that used $\epsilon_{\text{AMC}} = 20$.

To improve their throughput, several wireless communication systems use multiple frequency bands which simultaneously have a large frequency ratio. For instance, WLAN uses a lower frequency band of 2.4–2.485 GHz for the IEEE 802.11b/g Standard and two upper frequency bands of 5.15–5.35 and 5.725–5.875 GHz for the IEEE 802.11a Standard. The basic crossed multibranch dipole with a single-feed structure can be easily modified for use in these systems. As an example, a crossed trident-shaped dipole has been optimized to have CP radiation at the 2.4-/5.2-/5.8-GHz WLAN frequencies [80]. As shown

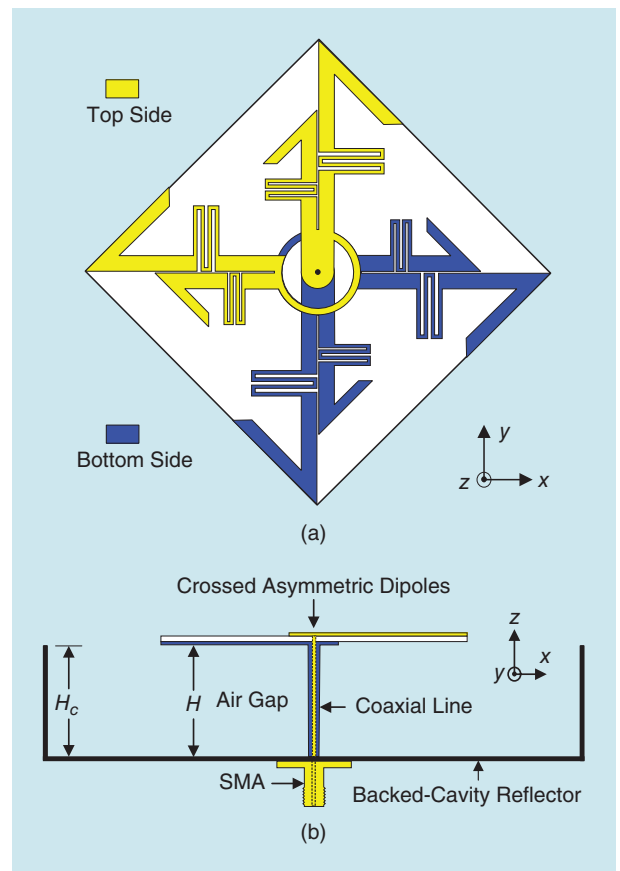


FIGURE 17. The dual-band CP, crossed asymmetric dipole antenna for GPS L1/L2 bands [76]. (a) Radiator. (b) Cross-sectional view. SMA: subminiature version A.

in Figure 20, the triband crossed dipoles are backed by a finite AMC surface to achieve low-profile, broadband characteristics, and a unidirectional radiation pattern at three bands. The AMC was designed to act as a PMC over the 2.4-GHz band, but perform like a PEC over the 5.2- and 5.8-GHz bands. In addition, the extra band generated by the surface waves propagating on the AMC was properly utilized to produce an improvement of the 3-dB AR bandwidth at the lower band. The fabricated prototype with an overall 2.4-GHz frequency size of approximately $0.576\lambda_o \times 0.576\lambda_o \times 0.14\lambda_o$ has a $|S_{11}| < -10\text{-dB}$ bandwidth of 2.21–2.62 GHz (410 MHz), 5.02–5.44 GHz (420 MHz), and 5.62–5.96 GHz (340 MHz) and a 3-dB AR bandwidth of 2.34–2.58 GHz (240 MHz), 5.14–5.38 GHz (240 MHz), and 5.72–5.88 GHz (160 MHz). In addition, the antenna system has a unidirectional RHCP gain pattern, high radiation efficiency, and stable operation over all three operating bands.

A novel AMC structure, which yields dual-frequency operation, has been employed as a reflector of a set of single-feed crossed asymmetric dipoles to achieve low profile and broadband characteristics for dual-band operation with a large frequency ratio [81]. Figure 21 shows the geometry of the low-profile dual-band antenna. The radiator was designed to produce CP radiation at the 2.4-/5.2-GHz bands. To match the operating frequencies of the radiator, the first and second resonances of the AMC structure were adjusted by using four T-shaped

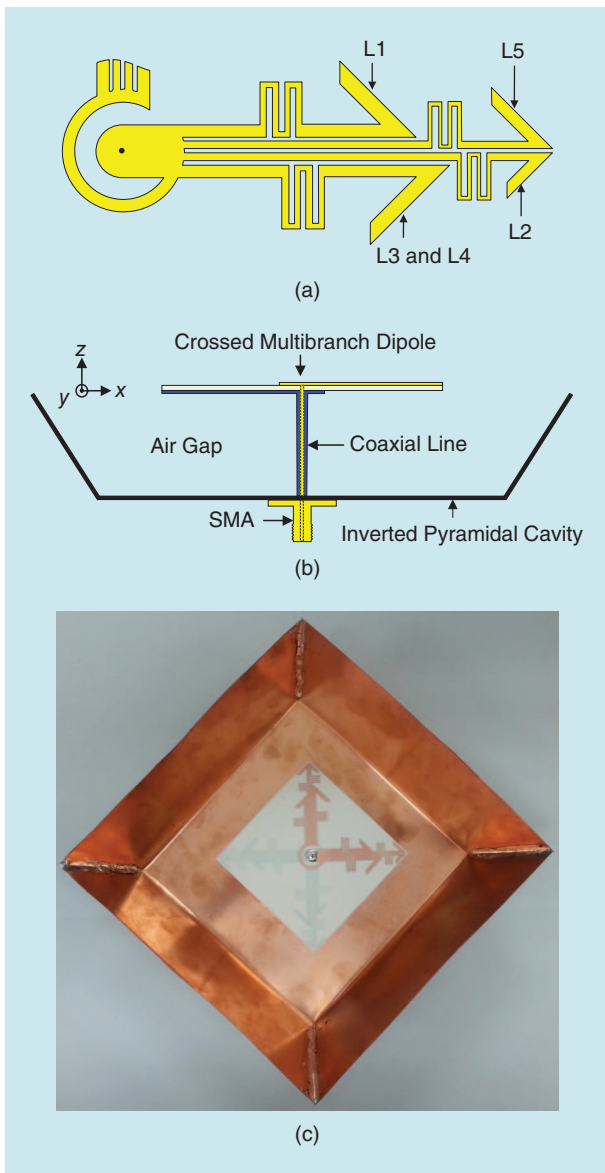


FIGURE 18. A multiband CP, crossed dipole antenna for GPS L1–L5 bands [78]. (a) The multibranch dipole arm and vacant-quarter printed ring. (b) A cross-sectional view. (c) The top view of the fabricated prototype. SMA: subminiature version A.

slits in each of the unit-cell patches, as shown in Figure 21(c). More importantly, the extra bands caused by the surface waves on the finite AMC surface were generated and consequently were utilized to improve the 3-dB AR bandwidths at both bands. The final design with an overall 2.4-GHz frequency size of $0.5760\lambda_o \times 0.576\lambda_o \times 0.088\lambda_o$ results in impedance bandwidths of 2.20–2.60 GHz (400 MHz) and 4.90–5.50 GHz (600 MHz) for $|S_{11}| < -1$ dB, 3-dB AR bandwidths of 2.30–2.50 GHz (20 MHz) and 5.05–5.35 GHz (30 MHz), as well as a highly efficient unidirectional radiation pattern. This antenna is a good candidate for dual-band wireless communications, such as WLAN, RFID, and WiMAX applications.

The interesting features of the AMC-based crossed dipole antennas are not only their ability to achieve high efficiency

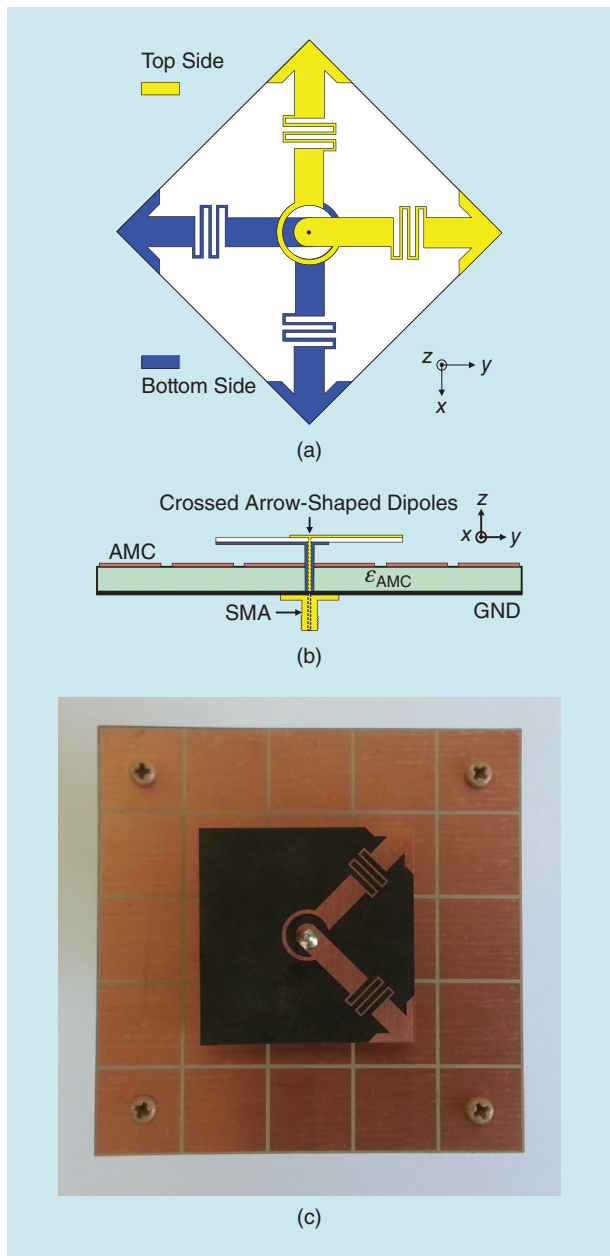


FIGURE 19. The low-profile CP crossed dipole integrated with a finite AMC surface for dual-band operation [79]. (a) A single-band radiator. (b) A cross-sectional view. (c) The top view of the fabricated prototype. SMA: subminiature version A. (Photo courtesy of Taylor & Francis.)

with a low profile, but also to generate additional resonances and the corresponding additional CP radiation features. These were utilized to add other operating bands or to broaden the antenna bandwidth. However, further investigations of these phenomena have not been rigorously pursued. The challenge is to develop a theoretical model that can be used to predict the extra resonances for all AMC-based antennas. Moreover, higher mode resonances exist in all of these antennas. Consequently, future work should consider the suppression or utilization of these resonances depending on whether or not they would be beneficial to the antenna in selected applications.

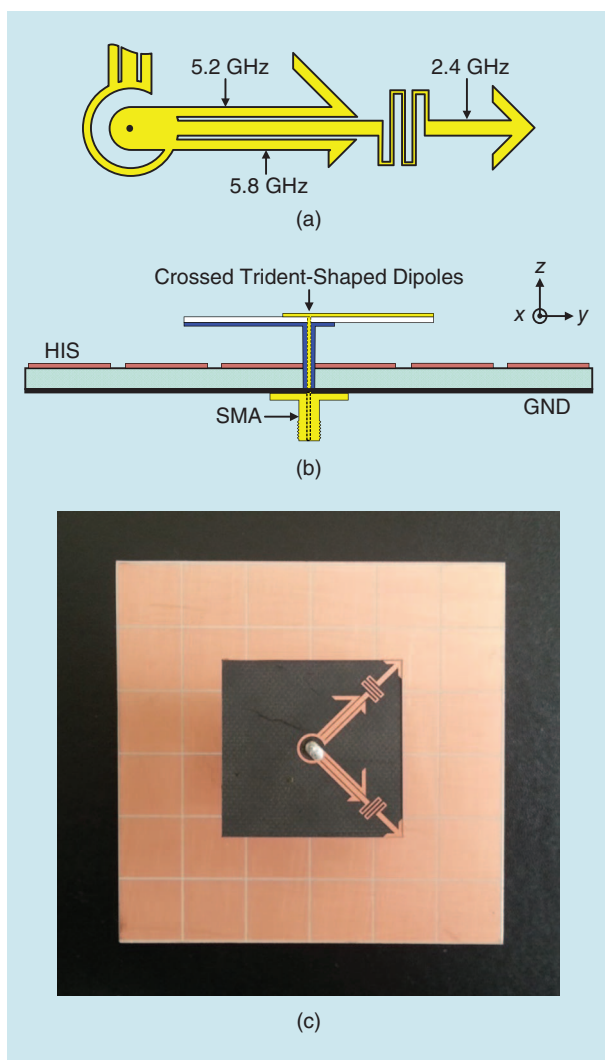


FIGURE 20. A CP crossed dipole antenna for 2.4-/5.2-/5.8-GHz WLAN applications [80]. (a) Trident-shaped dipole arm and vacant-quarter printed ring. (b) Cross-sectional view. (c) Top view of the fabricated prototype. SMA: subminiature version A.

CONCLUSIONS

A review of the designs, characteristics, and applications of crossed dipole antennas was presented, and we discussed why dual-feed crossed dipoles have been installed in many broadband antennas. In particular, they can be designed to radiate isotropic, omnidirectional, unidirectional CP, and unidirectional DP radiation. By a proper choice of the two orthogonal dipole lengths, it was described how CP radiation can be obtained with a single-feed structure. Some recent developments with the single-feed CP designs, including miniaturization, bandwidth enhancements, multiband operation, and radiation pattern control, also were reviewed. We illustrated how each dipole arm has been divided into multibranches with different lengths to achieve multiple resonances and how meander lines with modified trace ends have been inserted into each branch to achieve compact sizes. We also described how these compact radiators can easily be combined with different reflectors, namely, planar metallic, cavity-backed,

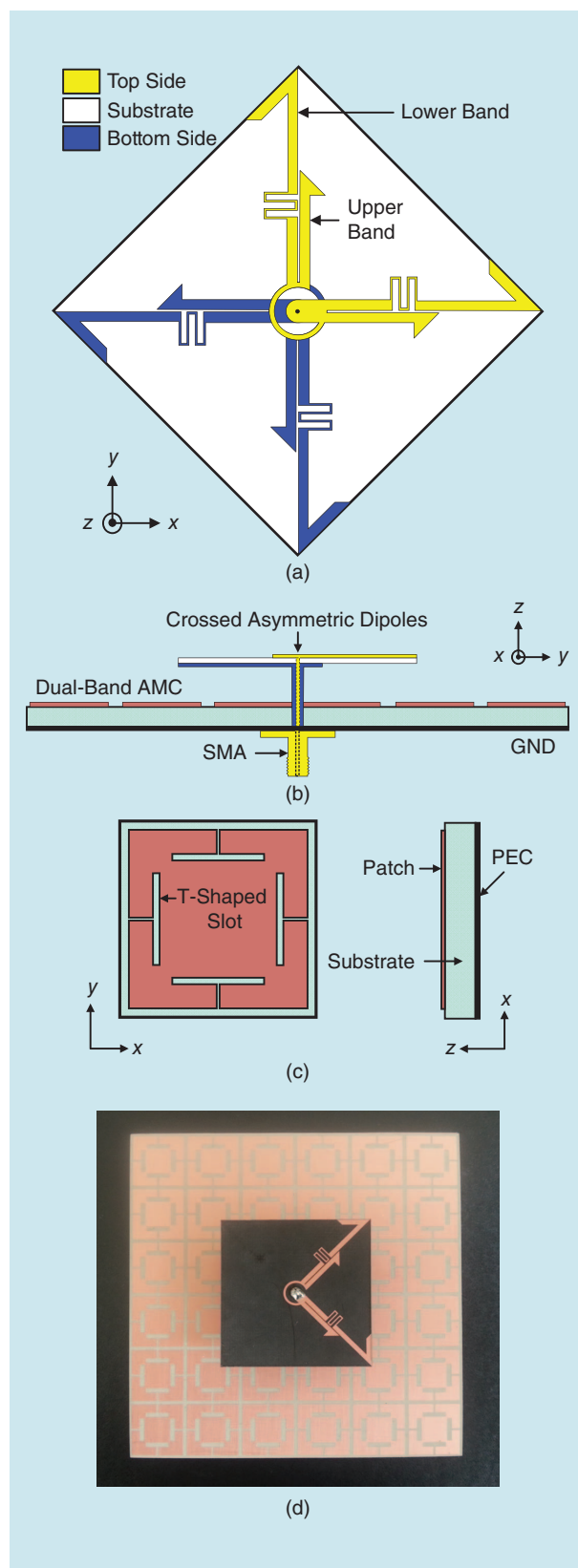


FIGURE 21. A CP crossed asymmetric dipole antenna integrated with a dual-band AMC surface [81]. (a) Radiator. (b) Cross-sectional view. (c) Unit cell of the dual-band AMC. (d) Top view of the fabricated prototype. SMA: subminiature version A.

and AMC surfaces, to achieve broadband and unidirectional radiation patterns. With their many desirable performance characteristics, cross-dipole-based antennas can be widely applied in many current and next-generation wireless communication systems.

Future research on crossed dipole antennas will be redirected by their recent developments, including simple feed structures, radiation pattern control, and profile miniaturization, as well as bandwidth enhancement. To simplify the feeding structure, single-feed antennas have been developed. Nonetheless, considerable research still needs to be done to achieve wideband and widebeam CP radiation. For profile miniaturization, crossed dipole radiators have been suspended above AMC surfaces instead of metallic reflectors. However, improvements in the AMC bandwidth need further consideration. Furthermore, the phenomena of extra resonances and their corresponding CP radiation features need rigorous investigation. With the recent progress reviewed in this article, there is great hope that more engineering approaches will be developed to tailor the crossed dipole antenna design to provide additional degrees of freedom and better performance characteristics for many wireless communication systems.

ACKNOWLEDGMENT

This work was supported by Information and Communication Technology Research and Development Program of MSIP/IITP (number 14-911-01-001).

AUTHOR INFORMATION

Son Xuat Ta (tasonxuata@ajou.ac.kr) earned his B.S. degree in electronics and telecommunications from Hanoi University of Science and Technology, Vietnam, in 2008. He is currently pursuing a Ph.D. degree with the Department of Electrical and Computer Engineering, Ajou University, Suwon, South Korea. His research is focused on wideband, multiband, circularly polarized, and metamaterial-based antennas for next-generation wireless communication systems.

Ikmo Park (ipark@ajou.ac.kr) received his B.S. degree in electrical engineering from the State University of New York at Stony Brook, and his M.S. and Ph.D. degrees in electrical engineering from the University of Illinois at Urbana-Champaign. He joined the Department of Electrical and Computer Engineering at Ajou University in March 1996. Before joining Ajou University, he worked with the Device & Materials Laboratory of LG Corporate Institute of Technology, Seoul, South Korea, where he was engaged in research and development of various antennas for personal communication systems, wireless local area networks, and direct broadcasting systems. He has authored or coauthored more than 250 technical journal and conference papers. He also holds more than 30 patents. His current research interests include the design and analysis of microwave, millimeter wave, terahertz wave, and nano-structured antennas. He is also a member of Eta Kappa Nu and Tau Beta Pi.

Richard W. Ziolkowski (ziolkowski@ece.arizona.edu) earned his B.S. degree in 1974 from Brown University, Providence, Rhode Island, and his M.S. and Ph.D. degrees, respectively, in 1975 and 1980 from the University of Illinois at Urbana-Champaign, all in physics. He is the Litton Industries

John M. Leonis Distinguished Professor in the Department of Electrical and Computer Engineering and a professor in the College of Optical Sciences at the University of Arizona. He was awarded an honorary doctorate, Doctor Technicus Honoris Causa, from the Technical University of Denmark in 2012. He was the 2014–2015 Australian Defence Science and Technology Organization (DSTO) Fulbright Distinguished Chair in Advanced Science and Technology and worked with the DSTO Aerospace Composite Technologies Group in Melbourne, Australia. He is a Fellow of the IEEE and the Optical Society of America. He served as the president of the IEEE Antennas and Propagation Society in 2005.

REFERENCES

- [1] G. Brown, "The turnstile," *Electron.*, vol. 9, pp. 14–17, Apr. 1936.
- [2] G. Brown and J. Epstein, "A pretuned Turnstile antenna," *Electron.*, vol. 18, pp. 102–107, June 1945.
- [3] P. Smith, "Cloverleaf antenna for F. M. broadcasting," *IRE Proc.*, vol. 35, no. 12, pp. 1556–1563, Dec. 1947.
- [4] R. Masters, "The super turnstile," *Broadcast News*, vol. 42, pp. 42–44, Jan. 1946.
- [5] G. J. Phillips, "V.H.F. aerials for television broadcasting," *IEE Proc.*, vol. 102, no. 5, pp. 687–688, Sept. 1955.
- [6] H. Kawakami, G. Sato, and R. Masters, "Characteristics of TV transmitting batwing antennas," *IEEE Trans. Antennas Propag.*, vol. 32, no. 12, pp. 1318–1326, Dec. 1984.
- [7] G. Sato and H. Kawakami, "Research on transmitting antennas," *IEEE Antennas Propag. Soc. Newslett.*, vol. 31, no. 3, pp. 5–12, June 1989.
- [8] "Batwing antennas radiate high power television signals," *Electr. Engin.*, vol. 57, no. 3, pp. 304–305, Mar. 1956.
- [9] O. Ben-dov, "New Turnstile antennas for horizontal and circular polarization," *IEEE Trans. Broadcast.*, vol. BC-22, no. 1, pp. 1–5, Mar. 1976.
- [10] R. N. Clark, "The fan vee circularly polarized TV antenna," *IEEE Trans. Broadcast.*, vol. BC-24, no. 1, pp. 20–22, Mar. 1978.
- [11] D. Hymas, "A new high power circularly polarized FM antenna," *IEEE Trans. Broadcast.*, vol. BC-25, no. 1, pp. 20–22, Mar. 1979.
- [12] H. Kawakami, "A review of and new results for broadband antennas for digital terrestrial broadcasting: The modified batwing antenna," *IEEE Antennas Propag. Mag.*, vol. 52, no. 5, pp. 78–88, Oct. 2010.
- [13] I. Radnovic, A. Nestic, and B. Milovanovic, "A new type of turnstile antenna," *IEEE Antennas Propag. Mag.*, vol. 52, no. 5, pp. 168–171, Oct. 2010.
- [14] G. Pan, Y. Li, Z. Zhang, and Z. Feng, "Isotropic radiation from a compact planar antenna using two crossed dipoles," *IEEE Antennas Wireless Propag. Lett.*, vol. 11, pp. 1338–1341, Nov. 2012.
- [15] I.-J. Yoon and H. Ling, "Design of an electrically small circularly polarised turnstile antenna and its application to near-field wireless power transfer," *IET Microwave Antennas Propag.*, vol. 8, no. 5, pp. 308–314, Apr. 2014.
- [16] S. G. M. Darwish, K. F. A. Hussein, and H. A. Mansour, "Circularly polarized crossed-dipole turnstile antenna for satellites," in *Proc. 21st Radio Science Conf.*, Mar. 16–18, 2004, pp. B17–1–15.
- [17] J.-M. Baracco, L. Salghetti-Drioli, and P. Maagt, "AMC low profile wideband reference antenna for GPS and GALILEO systems," *IEEE Trans. Antennas Propag.*, vol. 56, no. 8, pp. 2540–2547, Aug. 2008.
- [18] R. Wakabayashi, K. Shimada, H. Kawakami, and G. Sato, "Circularly polarized log-periodic dipole antenna for EMI measurements," *IEEE Trans. Electromagn. Compat.*, vol. 41, no. 2, pp. 93–99, May 1999.
- [19] G. Liu, L. Xu, and Z. Wu, "Miniaturised wideband circularly-polarised log-periodic Koch fractal antenna," *Electron. Lett.*, vol. 49, no. 21, pp. 1315–1316, Oct. 2013.
- [20] L. Xu, Y. Wang, and C. Gu, "Tri-band circularly-polarised antenna for CERTO application," *Electron. Lett.*, vol. 47, no. 2, pp. 86–87, Jan. 2011.
- [21] R. E. Fisk and J. A. Donovan, "A new CP antenna for television broadcast service," *IEEE Trans. Broadcast.*, vol. BC-25, no. 1, pp. 20–22, Mar. 1979.
- [22] R. K. Zimmerman, "Crossed dipoles fed with a turnstile network," *IEEE Trans. Microwave Theory Tech.*, vol. 46, no. 12, pp. 2151–2156, Dec. 1998.
- [23] F. Scire-Scappuzzo and S. N. Makarov, "A low-multipath wideband GPS antenna with cutoff or non-cutoff corrugated ground plane," *IEEE Trans. Antennas Propag.*, vol. 57, no. 1, pp. 33–46, Jan. 2009.
- [24] K. M. Mak and K. M. Luk, "A circularly polarized antenna with wide axial ratio bandwidth," *IEEE Trans. Antennas Propag.*, vol. 57, no. 10, pp. 3309–3312, Oct. 2009.
- [25] S.-W. Qu, C. H. Chan, and Q. Xue, "Wideband and high-gain composite cavity-backed crossed triangular bowtie dipoles for circular polarized radiation," *IEEE Trans. Antennas Propag.*, vol. 58, no. 10, pp. 3157–3164, Oct. 2010.
- [26] L. Wang, H.-C. Yang, and Y. Li, "Design of a new printed dipole antenna using in high latitudes for Inmarsat," *IEEE Antennas Wireless Propag. Lett.*, vol. 10, pp. 358–360, Apr. 2011.

- [27] J. Zhang, H. C. Yang, and D. Yang, "Design of a new high-gain circularly polarized antenna for inmarsat communications," *IEEE Antennas Wireless Propag. Lett.*, vol. 11, pp. 350–353, Mar. 2012.
- [28] Z.-Y. Zhang, N.-W. Liu, J.-Y. Zhao, and G. Fu, "Wideband circularly polarized antenna with gain improvement," *IEEE Antennas Wireless Propag. Lett.*, vol. 12, pp. 456–459, Mar. 2013.
- [29] E.-C. Choi, J. W. Lee, and T.-K. Lee, "Modified S-band satellite antenna with isoflux pattern and circularly polarized wide beamwidth," *IEEE Antennas Wireless Propag. Lett.*, vol. 12, pp. 1319–1322, Oct. 2013.
- [30] H. D. Hristov, H. Carrasco, R. Feick, and B. L. Ooi, "Low-profile X antenna with flat reflector for polarization diversity applications," *Microw. Opt. Technol. Lett.*, vol. 51, no. 6, pp. 1508–1512, June 2009.
- [31] H. D. Hristov, H. Carrasco, R. Feick, and G. Kirov, "Broadband two-port X antenna array with flat reflector for polarization diversity application," *Microw. Opt. Technol. Lett.*, vol. 52, no. 12, pp. 2833–2837, Dec. 2010.
- [32] J. Perruisseau-Carrier, T. W. Hee, and P. S. Hall, "Dual-polarized broadband dipole," *IEEE Antennas Wireless Propag. Lett.*, vol. 2, no. 1, pp. 310–312, 2003.
- [33] K.-M. Mak, H. Wong, and K.-M. Luk, "A shorted bowtie patch antenna with a cross dipole for dual polarization," *IEEE Antennas Wireless Propag. Lett.*, vol. 6, pp. 126–129, 2007.
- [34] B. Q. Wu and K.-M. Luk, "A broadband dual-polarized magneto-electric dipole antenna with simple feeds," *IEEE Antennas Wireless Propag. Lett.*, vol. 8, pp. 60–63, Dec. 2009.
- [35] L. Siu, H. Wong, and K.-M. Luk, "A dual-polarized magneto-electric dipole with dielectric loading," *IEEE Trans. Antennas Propag.*, vol. 57, no. 3, pp. 616–623, Mar. 2009.
- [36] Q. Xue, S. W. Liao, and J. H. Xu, "A differentially-driven dual-polarized magneto-electric dipole antenna," *IEEE Trans. Antennas Propag.*, vol. 61, no. 1, pp. 425–430, Jan. 2013.
- [37] F. Leon-Lerma, G. Ruvio, and M. J. Ammann, "A microstrip-fed printed crossed dipole for wireless applications," *Microw. Opt. Technol. Lett.*, vol. 48, no. 4, pp. 751–753, Apr. 2006.
- [38] J. A. Kasemodel and J. L. Volakis, "A planar dual linear-polarized antenna with integrated balun," *IEEE Antennas Wireless Propag. Lett.*, vol. 9, pp. 787–790, Aug. 2010.
- [39] Y.-H. Huang, Q. Wu, and Q.-Z. Liu, "Broadband dual-polarized antenna with high isolation for wireless communication," *Electron. Lett.*, vol. 45, no. 14, pp. 714–715, July 2009.
- [40] H. Huang, Z. Niu, B. Bai, and J. Zhang, "Novel broadband dual-polarized dipole antenna," *Microw. Opt. Technol. Lett.*, vol. 53, no. 1, pp. 148–150, Jan. 2011.
- [41] S.-G. Zhou, P.-K. Tan, and T.-H. Chio, "Low-profile, wideband dual-polarized antenna with high isolation and low cross polarization," *IEEE Antennas Wireless Propag. Lett.*, vol. 11, pp. 1032–1035, Aug. 2012.
- [42] B. Li, Y.-Z. Yin, Y. Ding, and Y. Zhao, "Wideband dual-polarized patch antenna with low cross polarization and high isolation," *IEEE Antennas Wireless Propag. Lett.*, vol. 11, pp. 427–430, Apr. 2012.
- [43] C. Liu, J.-L. Guo, Y.-H. Huang, and L.-Y. Zhou, "A novel dual-polarized antenna with high isolation and low cross polarization for wireless communication," *Prog. Electromagn. Res. Lett.*, vol. 32, pp. 129–136, 2012.
- [44] Y. Liu, H. Yi, H. Liu, and S.-X. Gong, "A novel dual-polarized dipole antenna with compact size for wireless communication," *Prog. Electromagn. Res. C*, vol. 40, pp. 217–227, 2013.
- [45] Y.-H. Huang, S.-G. Zhou, J.-L. Guo, and Y.-S. Chen, "Compact and wideband dual-polarized antenna with high isolation for wireless communication," *Prog. Electromagn. Res. Lett.*, vol. 38, pp. 171–180, May 2013.
- [46] W. Hu, Y. Z. Yin, P. Fei, and S. F. Zheng, "Design of a dual-polarized slot antenna with high isolation and low cross-polarization for wireless communication," *J. Electromagn. Waves Appl.*, vol. 26, no. 16, pp. 2185–2191, Nov. 2012.
- [47] W. Hu, X.-S. Ren, B. Li, Y.-Z. Yin, X. Yang, and J.-H. Yang, "Dual-band dual-polarized printed antenna for wireless communication," *J. Electromagn. Waves Appl.*, vol. 26, nos. 17–18, pp. 2242–2248, Oct. 2012.
- [48] Z. R. Li, L. Y. Chen, H. Zhang, Q. X. Guo, X. Q. Zhang, X. F. Wu, J. H. Wang, and Y. Yang, "Dual-polarized patch antenna with high isolation for DTV application," *J. Electromagn. Waves Appl.*, vol. 27, no. 14, pp. 1759–1766, 2013.
- [49] B. Li, W. Hu, J. Ren, and Y.-Z. Yin, "Low-profile dual-polarized patch antenna with HIS reflector for base station application," *J. Electromagn. Waves Appl.*, vol. 28, no. 8, pp. 956–962, 2014.
- [50] Y. Liu, H. Yi, F.-W. Wang, and S.-X. Gong, "A novel miniaturized broadband dual-polarized dipole antenna for base station," *IEEE Antennas Wireless Propag. Lett.*, vol. 12, pp. 1335–1338, Oct. 2013.
- [51] Z. Bao, Z. Nie, and X. Zong, "A novel broadband dual-polarization antenna utilizing strong mutual coupling," *IEEE Trans. Antennas Propag.*, vol. 62, no. 1, pp. 450–454, Jan. 2014.
- [52] M. F. Bolster, "A new type of circular polarizer using crossed dipoles," *IRE Trans. Microwave Theory Tech.*, vol. 9, no. 5, pp. 385–388, Sept. 1961.
- [53] B. Y. Toh, R. Cahill, and V. F. Fusco, "Understanding and measuring circular polarization," *IEEE Trans. Educ.*, vol. 46, no. 3, pp. 313–318, Aug. 2003.
- [54] K. Maamria and T. Nakamura, "Simple antenna for circular polarisation," *IEE Proc.-H*, vol. 139, no. 2, pp. 157–158, Apr. 1992.
- [55] Y. Kazama, "One-point feed printed crossed dipole with a reflector antenna combined with a reactively loaded parasitic loop for land mobile satellite communication antennas," *IEE Proc.-H*, vol. 140, no. 5, pp. 417–420, Oct. 1993.
- [56] J. W. Baik, K.-J. Lee, W.-S. Yoon, T.-H. Lee, and Y.-S. Kim, "Circularly polarised printed crossed dipole antennas with broadband axial ratio," *Electron. Lett.*, vol. 44, no. 13, pp. 785–786, June 2008.
- [57] W.-S. Yoon, S.-M. Han, J.-W. Baik, S. Pyo, J. Lee, and Y.-S. Kim, "Crossed dipole antenna with switchable circular polarisation sense," *Electron. Lett.*, vol. 45, no. 14, pp. 717–718, July 2009.
- [58] J.-W. Baik, T.-H. Lee, S. Pyo, S.-M. Han, J. Jeong, and Y.-S. Kim, "Broadband circularly polarized crossed dipole with parasitic loop resonators and its arrays," *IEEE Trans. Antennas Propag.*, vol. 59, no. 1, pp. 80–88, Jan. 2011.
- [59] L. Sun, Y.-H. Sun, Y.-H. Huang, B.-H. Sun, and Q.-Z. Liu, "A novel wide band and broad beamwidth circularly polarized antenna," *J. Electromagn. Waves Appl.*, vol. 25, no. 10, pp. 1459–1470, 2011.
- [60] P. Arnold, "A circularly polarized octave-bandwidth unidirectional antenna using conical dipoles," *IEEE Trans. Antennas Propag.*, vol. 18, no. 5, pp. 696–698, Sept. 1970.
- [61] S. N. Makarov and R. Ludwig, "Analytical model for the split-coaxial balun and its application to a linearly-polarized dipole or a CP turnstile," *IEEE Trans. Antennas Propag.*, vol. 55, no. 17, pp. 1909–1918, July 2007.
- [62] Y. He, W. He, and H. Wong, "A Wideband circularly polarized cross-dipole antenna," *IEEE Antennas Wireless Propag. Lett.*, vol. 13, pp. 67–70, Jan. 2014.
- [63] K. Lau, H. Wong, and K. Luk, "A full-wavelength circularly polarized slot antenna," *IEEE Trans. Antennas Propag.*, vol. 54, no. 2, pp. 741–743, Feb. 2006.
- [64] R. Li, D. C. Thompson, J. Papapolymerou, J. Laskar, and M. Tentzeris, "A circularly polarized short backfire antenna excited by an unbalance-fed crossed aperture," *IEEE Trans. Antennas Propag.*, vol. 54, no. 3, pp. 852–859, Mar. 2006.
- [65] H.-M. Chen, Y.-K. Wang, Y.-F. Lin, and Z.-Z. Yang, "Single-layer crossed dipole antenna with circular polarization for handheld RFID reader," *Microw. Opt. Technol. Lett.*, vol. 53, no. 5, pp. 1172–1176, May 2011.
- [66] Y.-F. Lin, Y.-K. Wang, H.-M. Chen, and Z.-Z. Yang, "Circularly polarized crossed dipole antenna with phase delay lines for RFID handheld reader," *IEEE Trans. Antennas Propag.*, vol. 60, no. 3, pp. 1221–1227, Mar. 2012.
- [67] R. W. Ziolkowski, P. Jin, and C. C. Lin, "Metamaterial-inspired engineering of antennas," *IEEE Proc.*, vol. 99, no. 10, pp. 1720–1731, Oct. 2011.
- [68] C.-C. Lin, P. Jin, and R. W. Ziolkowski, "Multi-functional, magnetically-coupled, electrically small, near-field resonant parasitic wire antennas," *IEEE Trans. Antennas Propag.*, vol. 59, no. 3, pp. 714–724, Mar. 2011.
- [69] P. Jin and R. W. Ziolkowski, "Multi-frequency, linear and circular polarized, metamaterial-inspired, near-field resonant parasitic antennas," *IEEE Trans. Antennas Propag.*, vol. 59, no. 5, pp. 1446–1459, May 2011.
- [70] P. Jin, C.-C. Lin, and R. W. Ziolkowski, "Multifunctional, electrically small, planar near-field resonant parasitic antennas," *IEEE Antennas Wireless Propag. Lett.*, vol. 11, pp. 200–204, Feb. 2012.
- [71] P. Jin and R. W. Ziolkowski, "High directivity, electrically small, low-profile, near-field resonant parasitic antennas," *IEEE Antennas Wireless Propag. Lett.*, vol. 11, pp. 305–309, Mar. 2012.
- [72] I. Park, S. X. Ta, J. Han, and R. W. Ziolkowski, "Applications of circularly polarized crossed dipole antennas," in *Proc. Int. Workshop Antenna Technology*, Sydney, Australia, Mar. 2014, pp. 2–4.
- [73] S. X. Ta, H. Choo, and I. Park, "Planar, lightweight, circularly polarized crossed dipole antenna for handheld UHF RFID reader," *Microw. Opt. Technol. Lett.*, vol. 55, no. 8, pp. 1874–1878, Aug. 2013.
- [74] S. X. Ta, J. J. Han, R. W. Ziolkowski, and I. Park, "Wide-beam circularly polarized composite cavity-backed crossed scythe-shaped dipole," in *Proc. Asia-Pacific Microwave Conf.*, Seoul, South Korea, Nov. 2013, pp. 1085–1087.
- [75] S. X. Ta, J. J. Han, and I. Park, "Compact circularly polarized composite cavity-backed crossed dipole for GPS applications," *J. Electromagn. Eng. Sci.*, vol. 13, no. 1, pp. 44–49, Mar. 2013.
- [76] S. X. Ta, I. Park, and R. W. Ziolkowski, "Dual-band wide-beam crossed asymmetric dipole antenna for GPS application," *Electron. Lett.*, vol. 48, no. 25, pp. 1580–1581, Dec. 2012.
- [77] S. X. Ta, J. Han, R. W. Ziolkowski, and I. Park, "Wide-beam circularly polarized crossed scythe-shaped dipoles for global navigation satellite systems," *J. Electromagn. Eng. Sci.*, vol. 13, no. 4, pp. 224–232, Dec. 2013.
- [78] S. X. Ta, H. Choo, I. Park, and R. W. Ziolkowski, "Multi-band, wide-beam, circularly polarized, crossed, asymmetrically barbed dipole antennas for GPS applications," *IEEE Trans. Antennas Propag.*, vol. 61, no. 11, pp. 5771–5775, Nov. 2013.
- [79] S. X. Ta and I. Park, "Dual-band operation of a circularly polarized radiator on finite artificial magnetic conductor surface," *J. Electromagn. Waves Appl.*, vol. 28, no. 7, Mar. 2014.
- [80] S. X. Ta, I. Park, and R. W. Ziolkowski, "Circularly polarized crossed dipole on an HIS for 2.4/5.2/5.8-GHz WLAN applications," *IEEE Antennas Wireless Propag. Lett.*, vol. 12, pp. 1464–1467, Nov. 2013.
- [81] S. X. Ta and I. Park, "Dual-band low-profile crossed asymmetric dipole antenna on dual-band AMC surface," *IEEE Antennas Wireless Propag. Lett.*, vol. 13, pp. 587–590, Mar. 2014.

